

November 8, 2018

# Quasiparticle interference in an iron-based superconductor

S. Sykora<sup>1,2</sup>, and Piers Coleman<sup>1</sup><sup>1</sup>*Center for Materials Theory, Rutgers University, Piscataway, New Jersey 08854, USA*<sup>2</sup>*IFW Dresden, Institute for Theoretical Solid State Physics, P.O. Box 270116, D-01171 Dresden, Germany*

We develop a model for the effect of a magnetic field on quasiparticle interference in an iron-based superconductor. Recently, scanning tunneling experiments have been performed on Fe(Se,Te) to determine the relative sign of the superconducting gap from the magnetic-field dependence of quasiparticle scattering amplitudes. Using a simple two-band BCS model, we study three different cases of scattering in a spin-split spectrum. The dominant effect of a magnetic field in iron-based superconductors is caused by the Pauli limiting of conduction electrons. Thereby time reversal odd scattering is induced which enhances the sign-preserving and depresses the sign-reversing peaks in the quasiparticle interference patterns.

PACS numbers: 71.10.Fd, 71.30.+h

## I. INTRODUCTION

The discovery of iron-based layered pnictide and chalcogenide superconductors<sup>1</sup> with superconducting (SC) transition temperature as high as 55K (Ref.<sup>2</sup>) has generated enormous interest in the physics of these materials. Similar to the cuprates, the iron-based superconductors are highly two-dimensional and superconductivity occurs in close proximity to anti-ferromagnetic order,<sup>3</sup> leading several groups to propose that the pairing is driven by anti-ferromagnetic spin fluctuations.<sup>4-7</sup>

The first step in identifying the pairing mechanism is to investigate the structure of the SC-gap function, which describes the strength and quantum mechanical phase of electron pairs in momentum ( $\mathbf{k}$ ) space. While the SC gap function of conventional phonon-mediated superconductors has the same phase throughout momentum space (s-wave symmetry), that of spin-fluctuation mediated superconductors is expected to exhibit a sign reversal between those Fermi momenta connected by characteristic wave vector  $\mathbf{Q}$  of the spin fluctuations.<sup>8</sup> In  $d$  wave superconductors, the nodal planes of the order parameter intersect with the Fermi surface, leading to gapless quasiparticle (QP) excitations that can be detected thermodynamically and by low energy probes. However, if the sign reversal occurs between disconnected hole and electron pockets (compare Fig. 1) resulting in an “ $s_{\pm}$  symmetry,”<sup>4,5</sup> the relative sign of SC gap must be determined by phase-sensitive experiments such as Josephson junctions experiments<sup>9</sup> or composite SC loops.<sup>10</sup> An alternative technique is scanning tunneling microscopy (STM) which determines the dispersion of quasiparticle states from the quasiparticle interference (QPI) patterns induced by impurity scattering<sup>11-15</sup>. Such experiments, performed in an external magnetic field, offer the capability of probing the phase of the superconducting order parameter by detecting a field enhancement of the sign-preserving scattering that results from the sensitivity of QPI to the coherence factors associated with impurity scattering.

The recent detection of a field enhancement of quasiparticle scattering between the hole pockets of the iron chalcogenide superconductor Fe(Se,Te) has been interpreted<sup>16</sup> as evidence for the  $s_{\pm}$  pairing scenario. However, there are certain differences between the field effect in iron-based and cuprate superconductors that raise questions about this interpretation. For example, Fe(Se,Te) is a Pauli-limited superconductor where the coupling of the field to the conduction electrons becomes important. In this material, the Zeeman splitting is a large fraction of the superconducting gap size,  $\mu_B B / \Delta \approx 0.4$ , generating new components to the field-induced scattering that have been hitherto neglected in models of quasiparticle interference.

In the cuprates, quasiparticle scattering in external magnetic fields is strongly affected by vortices. However, STM measurements on Fe(Se,Te) did not observe appreciable correlation in space between the location of vortices and the magnitude of field-induced change in the QPI intensity.<sup>16</sup> These results suggest that in Pauli-limited superconductors the role of vortices is much less important compared to homogeneously distributed field-induced scatterers created by Zeeman splitting. One of the key arguments advanced in the STM measurements of Fe(Se,Te), is that an applied magnetic field will, in general, enhance the time-reverse odd components of the scattering that lead to sign-preserving scattering. How effective are these arguments in the presence of significant Pauli limiting effects, and to what extent can we attribute the observed field enhancement of the sign-preserving scattering to the Zeeman splitting?

Motivated by the above considerations, this paper develops a phenomenological model for the field-dependent QPI in iron-based superconductors, taking into account the Zeeman splitting of the quasiparticle dispersion. Using a simple two-band BCS model for an unconventional  $s$ -wave superconductor, we calculate the STM conductance ratio for different types of disorder in an external magnetic field at which we neglect the scattering off vortices. In our model, we assume an  $s_{\pm}$ -wave symmetry for

the superconducting order parameter which means that the size of the superconducting gap is isotropic along the hole and electron pockets. Our study confirms that Zeeman splitting provides a strong source of time-reversal-odd, sign-preserving scattering. We also find that if resonant or magnetic scatterers are present in the superconducting material, the spin split spectrum leads to an enhancement of sign preserving scattering. QPI patterns for non-magnetic and magnetic impurities without Zeeman field have been computed theoretically by a number of works using more realistic band structures.<sup>17-21</sup>

The paper is organized as follows. In Sec. II A, we briefly resume the basic concepts behind some types of scatterers with different time reversal symmetry properties and their coherence factors. The BCS model for an iron-based superconductor will be described in Sec. II B. After a short discussion about calculating the tunneling conductance from local density of states in Sec. III, we present our results of the numerical evaluation in Sec. IV. We conclude in Sec. V.

## II. PHENOMENOLOGICAL MODEL

### A. Coherence factors

An STM measurement probes quasiparticle interference (QPI) by observing Friedel oscillations in the tunneling density of states induced by impurity scattering. The Fourier transform of these fluctuations in the density of states provides information about the rate at which quasiparticles are scattered by impurities. In general, the rate of impurity scattering is proportional to the coherence factors associated with the underlying scattering mechanism. By measuring the momentum dependence of the scattering, it becomes possible to extract phase sensitive information about the underlying order parameter.

Quasiparticles in a superconductor are a coherent superposition of electrons and holes. Coherence factors describe the difference between the scattering rates of a SC quasiparticle and a bare electron off a given scatterer.<sup>22</sup> In general, the scattering rate of an electron from initial momentum  $\mathbf{k}$  to final momentum  $\mathbf{k}'$  is determined by an energy-dependent  $t$ -matrix  $\hat{T}(\mathbf{k}, \mathbf{k}', \omega)$ . The  $t$ -matrix, which depends on the quasiparticle spin degrees of freedom is most conveniently described using four-component Nambu notation<sup>23, 24</sup>. For a single impurity with scattering potential  $\hat{U}(\mathbf{k}, \mathbf{k}')$  in momentum space, the corresponding  $t$ -matrix exactly accounts for multiple scattering off that impurity.<sup>24, 25</sup> In first-order perturbation theory (Born approximation) the  $t$ -matrix is equal to  $\hat{U}(\mathbf{k}, \mathbf{k}')$ . In four-component Nambu notation the electron field is described by a four-component spinor containing particle and hole operators,<sup>23</sup>

$$\Psi_{\mathbf{k}}^{\dagger} = \begin{pmatrix} c_{\mathbf{k},\uparrow}^{\dagger} & c_{-\mathbf{k},\downarrow}^{\dagger} & c_{-\mathbf{k},\downarrow} & -c_{\mathbf{k},\uparrow} \end{pmatrix}, \quad (1)$$

where  $\mathbf{k}$  is the momentum.

We now review the connection between coherence factors for scattering in a BCS superconductor and the time-reversal symmetry of the scattering process. Consider a scattering process described by the  $t$ -matrix,

$$\hat{T} = \sum_{\mathbf{k}, \mathbf{k}'} \Psi_{\mathbf{k}}^{\dagger} \hat{T}_{\mathbf{k}, \mathbf{k}'} \Psi_{\mathbf{k}'}, \quad (2)$$

where the Nambu-spinors  $\Psi_{\mathbf{k}}^{\dagger}$  and  $\Psi_{\mathbf{k}'}$  account for different particle states according to Eq. (1). In the superconducting state, the  $t$ -matrix determines the Friedel oscillations in the local density of states that are probed in an STM experiment. To determine the matrix elements for quasiparticle scattering, we apply a Bogoliubov transformation to the particle spinors in Eq. (2), leading to

$$\begin{pmatrix} c_{\mathbf{k},\uparrow} \\ c_{-\mathbf{k},\downarrow} \\ c_{-\mathbf{k},\downarrow}^{\dagger} \\ -c_{\mathbf{k},\uparrow}^{\dagger} \end{pmatrix} = \begin{pmatrix} u_{\mathbf{k}} & 0 & v_{\mathbf{k}} & 0 \\ 0 & u_{\mathbf{k}} & 0 & v_{\mathbf{k}} \\ -v_{\mathbf{k}} & 0 & u_{\mathbf{k}} & 0 \\ 0 & -v_{\mathbf{k}} & 0 & u_{\mathbf{k}} \end{pmatrix} \begin{pmatrix} a_{\mathbf{k},\uparrow} \\ a_{-\mathbf{k},\downarrow} \\ a_{-\mathbf{k},\downarrow}^{\dagger} \\ -a_{\mathbf{k},\uparrow}^{\dagger} \end{pmatrix}, \quad (3)$$

where for convenience, we have assumed a gauge in which the Bogoliubov coefficients are real. For a BCS superconductor with electronic dispersion  $\varepsilon_{\mathbf{k}}$ , gap function  $\Delta_{\mathbf{k}}$  and quasiparticle energies  $E_{\mathbf{k}} = \sqrt{\varepsilon_{\mathbf{k}}^2 + \Delta_{\mathbf{k}}^2}$  the Bogoliubov coefficients are

$$u_{\mathbf{k}} = \sqrt{\frac{1}{2} \left( 1 + \frac{\varepsilon_{\mathbf{k}}}{E_{\mathbf{k}}} \right)}, \quad (4)$$

$$v_{\mathbf{k}} = \text{sign}(\Delta_{\mathbf{k}}) \sqrt{\frac{1}{2} \left( 1 - \frac{\varepsilon_{\mathbf{k}}}{E_{\mathbf{k}}} \right)}. \quad (5)$$

Introducing a Nambu spinor for the quasiparticle operators  $\Phi_{\mathbf{k}}^{\dagger} = (a_{\mathbf{k},\uparrow}^{\dagger} a_{-\mathbf{k},\downarrow}^{\dagger} a_{-\mathbf{k},\downarrow} - a_{\mathbf{k},\uparrow})$ , we may write the Bogoliubov transformation (3) as

$$\Psi_{\mathbf{k}} = (u_{\mathbf{k}} \hat{1} + i v_{\mathbf{k}} \hat{\tau}_2) \Phi_{\mathbf{k}}, \quad (6)$$

where  $\hat{1}$  is the  $4 \times 4$  unit matrix and  $\hat{\tau}_2$  is the isospin matrix,

$$\hat{\tau}_2 = i \begin{pmatrix} 0 & -1 \\ 1 & 0 \end{pmatrix}, \quad (7)$$

where an underscore denotes a two dimensional matrix. Using Eqs. (2) and (6) the  $t$ -matrix can be written in the form  $\hat{T} = \sum_{\mathbf{k}, \mathbf{k}'} \Phi_{\mathbf{k}}^{\dagger} \hat{T}_{\mathbf{k}, \mathbf{k}'}^{QP} \Phi_{\mathbf{k}'}$ , where

$$\hat{T}_{\mathbf{k}, \mathbf{k}'}^{QP} = (u_{\mathbf{k}} \hat{1} - i v_{\mathbf{k}} \hat{\tau}_2) \hat{T} (u_{\mathbf{k}'} \hat{1} + i v_{\mathbf{k}'} \hat{\tau}_2). \quad (8)$$

Equation (8) shows that the scattering matrix elements of  $\hat{T}_{\mathbf{k}, \mathbf{k}'}^{QP}$  of the SC quasiparticles are determined by combinations of the Bogoliubov coefficients  $u_{\mathbf{k}}$  and  $v_{\mathbf{k}}$ . Note that the sign of the SC order parameter  $\Delta_{\mathbf{k}}$  enters the coherence factors according to Eq. (5) so the momentum dependence of quasiparticle scattering is sensitive to the way the phase of  $\Delta_{\mathbf{k}}$  changes in momentum space.

$t$ -matrix	Scatterer	Coherence factor	Enhances	Time reversal
$\hat{\tau}_3$	Potential	$u_{\mathbf{k}}u_{\mathbf{k}'} - v_{\mathbf{k}}v_{\mathbf{k}'}$	$+-$	even
$\hat{\sigma}_3$	Magnetic	$u_{\mathbf{k}}u_{\mathbf{k}'} + v_{\mathbf{k}}v_{\mathbf{k}'}$	$++$	odd
$\hat{1} \times t_{odd}(\omega)$	Resonant	$u_{\mathbf{k}}u_{\mathbf{k}'} + v_{\mathbf{k}}v_{\mathbf{k}'}$	$++$	odd

TABLE I: Relation between coherence factors and time reversal symmetry properties for a set of particle conserving scatterers. In resonant scattering, the  $t$ -matrix is an odd-function of frequency  $t_{odd}(\omega) = -t_{odd}(-\omega)$ .

Now the action of the  $\hat{\tau}_2$  matrix on the  $t$ -matrix is closely related to its transformation under time reversal. The time-reversed  $t$ -matrix  $\hat{T}_{\mathbf{k},\mathbf{k}'}^\theta$  is determined from its transpose in the following way:

$$\hat{T}_{\mathbf{k},\mathbf{k}'}^\theta(\omega) = \hat{\sigma}_2 \hat{T}_{-\mathbf{k}',-\mathbf{k}}^T(-\omega) \hat{\sigma}_2, \quad (9)$$

where for generality, we have included the frequency dependence of the  $t$ -matrix. Now since the Nambu spinors satisfy the relation  $\Psi_{-\mathbf{k}}^* = (\Psi_{-\mathbf{k}}^\dagger)^T = \hat{\sigma}_2 \hat{\tau}_2 \Psi_{\mathbf{k}}$ , it follows from Eq. (2) that an arbitrary  $t$ -matrix satisfies the ‘‘CPT’’ relation

$$\hat{\tau}_2 \hat{\sigma}_2 \hat{T}_{-\mathbf{k}',-\mathbf{k}}^T(-\omega) \hat{\sigma}_2 \hat{\tau}_2 = -\hat{T}_{\mathbf{k},\mathbf{k}'}(\omega).$$

Combining these two relations, it follows that the time-reversed  $t$ -matrix is given by

$$\hat{T}_{\mathbf{k},\mathbf{k}'}^\theta(\omega) = -\hat{\tau}_2 \hat{T}_{\mathbf{k},\mathbf{k}'}(\omega) \tau_2,$$

so that if the  $t$ -matrix has a well-defined parity  $\theta$  under time-reversal  $\hat{T}_{\mathbf{k},\mathbf{k}'}^\theta = \theta \hat{T}_{\mathbf{k},\mathbf{k}'}$ , it follows that

$$\theta \hat{T}_{\mathbf{k},\mathbf{k}'}(\omega) = -\hat{\tau}_2 \hat{T}_{\mathbf{k},\mathbf{k}'}(\omega) \hat{\tau}_2.$$

With this relationship, we can rewrite the quasiparticle  $t$ -matrix in the form

$$\begin{aligned} \hat{T}_{\mathbf{k},\mathbf{k}'}^{QP} &= (u_{\mathbf{k}}u_{\mathbf{k}'} - \theta v_{\mathbf{k}}v_{\mathbf{k}'}) \hat{T}_{\mathbf{k},\mathbf{k}'} \\ &+ (v_{\mathbf{k}}u_{\mathbf{k}'} + \theta v_{\mathbf{k}'}u_{\mathbf{k}}) (-i\hat{\tau}_2) \hat{T}_{\mathbf{k},\mathbf{k}'}. \end{aligned} \quad (10)$$

It is the *diagonal elements* of this matrix that determine quasiparticle scattering. If we restrict our attention to

scattering processes that preserve particle number, then the second term in this expression is off-diagonal in the quasiparticle basis, and does not contribute to low-energy quasiparticle scattering. In this case, the quasiparticle scattering matrix is determined by the diagonal elements of

$$\begin{aligned} \hat{T}_{\mathbf{k},\mathbf{k}'}^{QP} &= (u_{\mathbf{k}}u_{\mathbf{k}'} - \theta v_{\mathbf{k}}v_{\mathbf{k}'}) \hat{T}_{\mathbf{k},\mathbf{k}'} \\ &\text{(particle-conserving scattering)} \end{aligned} \quad (11)$$

Near the Fermi surface, the magnitudes of the Bogoliubov coefficients are equal  $|u_{\mathbf{k}_F}| = |v_{\mathbf{k}_F}| = \frac{1}{\sqrt{2}}$ , so that near the Fermi surface,

$$\hat{T}_{\mathbf{k},\mathbf{k}'}^{QP} \propto (1 - \theta \text{sgn}(\Delta_{\mathbf{k}}\Delta_{\mathbf{k}'})) \quad (12)$$

In other words, time-reverse even scattering ( $\theta = 1$ ), gives rise to sign-reversing scattering, while time-reverse odd scattering ( $\theta = -1$ ) gives rise to sign-preserving scattering.

Cases of particular interest are potential, magnetic and resonant scattering, respectively denoted by  $t$ -matrices of the form  $\hat{\tau}_3$ ,  $\hat{\sigma}_3$ , and  $\hat{1} \times t_{odd}(\omega)$ , ( where  $t_{odd}(\omega) = -t_{odd}(-\omega)$  denotes an odd function of frequency). The coherence factors and time-reversal parities corresponding to these scattering mechanisms are listed in Table I. The application of a magnetic field selectively enhances time-reversal odd scattering. We now describe a theoretical model for the field-dependent scattering of quasiparticles in an  $s_{\pm}$  superconductor.

## B. BCS model of a Pauli-limited $s_{\pm}$ superconductor

The Fermi surface of iron-based superconductors consists of two-dimensional hole and electron pockets centered at  $\Gamma$  and M points, respectively.<sup>26</sup> A schematic picture of the disconnected Fermi surface is shown in Fig. 1. Since the hole and the electron pockets are similar in both shape and volume, the interband nesting between these pockets may generate spin fluctuations at momentum  $\mathbf{Q} = (\pi, 0)$  which can be detected as a coherence

peak at  $\mathbf{Q}$  in the Fourier-transformed local density of states. If such a spin fluctuation induces the electron pairing, a sign reversal of the SC-gap function occurs between the hole and electron pockets, resulting in  $s_{\pm}$ -wave symmetry.<sup>4-7</sup>

We employ a simple two-band tight binding model with a singlet pairing. In our model, we assume an extreme Pauli-limited superconductor, in which the dominant effects of the applied magnetic field enter through the Zeeman splitting of the conduction sea. In our simplified

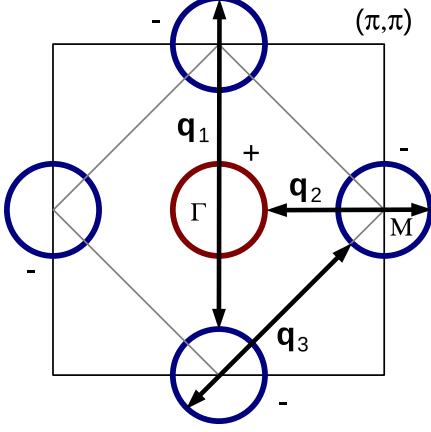


FIG. 1: Schematic picture of the disconnected Fermi surface of an iron-based superconductor. For simplicity, two hole cylinders and two electron cylinders around  $\Gamma$  and  $M$  points are represented as circles. Signs of the SC gap expected for  $s_{\pm}$ -wave symmetry are denoted as '+' and '-' in the picture. Arrows denote inter-Fermi-pocket scatterings. The wavevectors  $\mathbf{q}_1$  and  $\mathbf{q}_3$  are "sign-preserving", connecting pockets with the same superconducting phase, while  $\mathbf{q}_2$  is "sign-reversing", connecting pockets with opposite superconducting phase.

treatment, we assume that these effects are strong enough to permit us to neglect orbital effects of the field.

The model Hamiltonian is then

$$\mathcal{H} = \sum_{\mathbf{k}, \sigma} \left( \varepsilon_{\mathbf{k}, \sigma}^c c_{\mathbf{k}, \sigma}^\dagger c_{\mathbf{k}, \sigma} + \varepsilon_{\mathbf{k}, \sigma}^d d_{\mathbf{k}, \sigma}^\dagger d_{\mathbf{k}, \sigma} \right) - \sum_{\mathbf{k}} \left[ \Delta_{\mathbf{k}} \left( c_{\mathbf{k}, \uparrow}^\dagger c_{-\mathbf{k}, \downarrow}^\dagger + d_{\mathbf{k}, \uparrow}^\dagger d_{-\mathbf{k}, \downarrow}^\dagger \right) + \text{h.c.} \right], \quad (13)$$

where 'c' and 'd' denote the two electron bands describing an electron pocket at  $M$  point and a hole pocket at  $\Gamma$  point, respectively. We model the Fermi surface with the following dispersion

$$\varepsilon_{\mathbf{k}, \sigma}^c = 2t [\cos(k_x + k_y) + \cos(k_x - k_y)] + \mu_c - \sigma \mu_B B \quad (\text{electron pocket at } M \text{ point}), \quad (14)$$

$$\varepsilon_{\mathbf{k}, \sigma}^d = 2t (\cos k_x + \cos k_y) - \mu_d - \sigma \mu_B B \quad (\text{hole pocket at } \Gamma \text{ point}), \quad (15)$$

where  $\mu_B$  is the Bohr Magneton. Note that here, all orbital effects of the magnetic field on the dispersion and gap function have been neglected. Finally, we assume a superconducting field of  $s_{\pm}$ -wave symmetry described by the gap function

$$\Delta_{\mathbf{k}} = \tilde{\Delta} [\cos(k_x + k_y) + \cos(k_x - k_y)] = 2\tilde{\Delta} \cos k_x \cos k_y. \quad (16)$$

In the numerical work reported here, we took values  $\mu_c = 3.56t$ ,  $\mu_d = 3.2t$ , and  $\tilde{\Delta} = 0.2t$ . With these parameters, the minimum value quasiparticle gap on the Fermi surface is given by  $\Delta = 1.6\tilde{\Delta} = 0.32t$ .

### III. TUNNELING CONDUCTANCE

Following the ideas of Ref.<sup>27</sup> in this section we numerically model the conductance ratio measured by an STM experiment<sup>28</sup>. First, we review the relation between tunneling conductance and the local density of states (LDOS). Within a simplified model of the tunneling process, the differential tunneling conductance  $dI/dV(\mathbf{r}, V)$  at a location  $\mathbf{r}$  and Voltage  $V$  is given by

$$\frac{dI}{dV}(\mathbf{r}, V) \propto |M(\mathbf{r})|^2 \rho(\mathbf{r}, eV), \quad (17)$$

where  $\rho(\mathbf{r}, \omega) = A(\mathbf{r}, \mathbf{r}, \omega)$  is the single-particle density of states at energy  $\omega$  and  $M(\mathbf{r})$  is the spatially dependent tunneling-matrix element, which includes contributions of the sample wave function around the tip. Thus, the tunneling conductance measures the thermally smeared LDOS of the sample at the position  $\mathbf{r}$  of the tip. Note that a spatial dependence of the LDOS often arises from a scattering off impurities distributed in the sample.

To filter out the spatial variations in the tunneling-matrix elements  $M(\mathbf{r})$ , the conductance ratio is taken as

$$Z(\mathbf{r}, V) = \frac{\frac{dI}{dV}(\mathbf{r}, +V)}{\frac{dI}{dV}(\mathbf{r}, -V)} = \frac{\rho_0(eV) + \delta\rho(\mathbf{r}, eV)}{\rho_0(-eV) + \delta\rho(\mathbf{r}, -eV)}. \quad (18)$$

The first part  $\rho_0(\pm eV)$  of the LDOS describes the sample-averaged tunneling density of states at bias voltage  $\pm V$ . The spatial fluctuations of  $\rho(\mathbf{r}, \pm eV)$  are given by the second part  $\delta\rho(\mathbf{r}, \pm eV)$ . For small fluctuations  $\delta\rho(\mathbf{r}, \pm eV) \ll \rho_0(\pm eV)$  the Fourier transform of expression (18) is

$$Z(\mathbf{q}, V) = Z_0(V)(2\pi)^2 \delta(\mathbf{q}) + Z_0(V) \left[ \frac{\delta\rho(\mathbf{q}, eV)}{\rho_0(eV)} - \frac{\delta\rho(\mathbf{q}, -eV)}{\rho_0(-eV)} \right], \quad (19)$$

where  $Z_0(V) = \frac{\rho_0(eV)}{\rho_0(-eV)}$ . The Fourier transformed conductance ratio  $Z(\mathbf{q}, V)$  consists of a single delta function term at  $\mathbf{q} = 0$  and a background, which describes the interference patterns produced by quasiparticle scattering off impurities. The condition for small fluctuations is satisfied in the clean limit at finite and sufficiently large bias voltages  $|V| > 0$ .<sup>27</sup>

It proves useful to write the fluctuations in the conductance ratio as a sum of two terms, even and odd in the bias voltage

$$Z(\mathbf{q}, V)|_{\mathbf{q} \neq 0} = Z_0(V) \left\{ \delta\rho^+(\mathbf{q}, eV) \left[ \frac{1}{\rho_0(eV)} - \frac{1}{\rho_0(-eV)} \right] + \delta\rho^-(\mathbf{q}, eV) \left[ \frac{1}{\rho_0(eV)} + \frac{1}{\rho_0(-eV)} \right] \right\}, \quad (20)$$

where  $\delta\rho^\pm(\mathbf{q}, \omega) = [\delta\rho(\mathbf{q}, +\omega) \pm \delta\rho(\mathbf{q}, -\omega)]/2$ . Depending on the particle-hole symmetry properties of the sample-averaged tunneling density of states  $\rho_0(V)$ , one of these terms can dominate.

We calculate the fluctuations of the LDOS in Eq. (20) using the Green's function of a superconductor in the presence of impurities. As is discussed in Sec. II, the electron field inside a superconductor can be described by a four-component vector which is written as

$$\Psi^\dagger(\mathbf{r}, \tau) = \left( \psi_\uparrow^\dagger(\mathbf{r}, \tau), \psi_\downarrow^\dagger(\mathbf{r}, \tau), \psi_\downarrow(\mathbf{r}, \tau), -\psi_\uparrow(\mathbf{r}, \tau) \right) \quad (21)$$

in real space, where  $\mathbf{r}$  denotes the position vector and  $\tau$  is imaginary time. The matrix Green's function is defined as the time-ordered average,

$$\hat{G}_{\alpha\beta}(\mathbf{r}', \mathbf{r}; \tau) = -\langle T_\tau \Psi_\alpha(\mathbf{r}', \tau) \Psi_\beta^\dagger(\mathbf{r}, 0) \rangle. \quad (22)$$

For an electronic system in the presence of impurities, the Green's function (22) is usually calculated using the  $t$ -matrix method.<sup>24,25</sup> As is already discussed above, for a single impurity with scattering potential  $\hat{U}$ , the  $t$ -matrix exactly accounts for multiple scattering off that impurity. In momentum space, the  $t$ -matrix is determined by the following self-consistent equation:

$$\begin{aligned} \hat{T}(\mathbf{k}, \mathbf{k}', \omega) &= \hat{U}(\mathbf{k}, \mathbf{k}') \\ &+ \sum_{\mathbf{k}''} \hat{U}(\mathbf{k}, \mathbf{k}'') \hat{G}_0(\mathbf{k}'', \omega) \hat{T}(\mathbf{k}'', \mathbf{k}', \omega), \end{aligned} \quad (23)$$

where  $\hat{U}(\mathbf{k}, \mathbf{k}')$  is the scattering potential of a single impurity and  $\hat{G}_0(\mathbf{k}, \omega)$  is the bare Green's function of the BCS superconductor without impurities. The Green's function for an electron with a normal-state dispersion  $\varepsilon_{\mathbf{k}}$  and gap function  $\Delta_{\mathbf{k}}$  in an external magnetic field  $B$  is

$$\hat{G}_0(\mathbf{k}, \omega) = [\omega \hat{1} - \varepsilon_{\mathbf{k}} \hat{\tau}_3 - B \hat{\sigma}_3 - \Delta_{\mathbf{k}} \hat{\tau}_1]^{-1}. \quad (24)$$

Using  $\hat{G}_0(\mathbf{k}, \omega)$  and Eq. (23), the Fourier transformed Green's function can be written as

$$\hat{G}(\mathbf{k}, \mathbf{k}', \omega) = \hat{G}_0(\mathbf{k}, \omega) + \hat{G}_0(\mathbf{k}, \omega) \hat{T}(\mathbf{k}, \mathbf{k}', \omega) \hat{G}_0(\mathbf{k}', \omega). \quad (25)$$

Note that since translational invariance is broken by impurities, the Green's function depends on two momenta,  $\mathbf{k}$  and  $\mathbf{k}'$ .

The LDOS is determined by the analytic continuation  $\hat{G}(\mathbf{r}', \mathbf{r}; i\omega_n) \rightarrow \hat{G}(\mathbf{r}', \mathbf{r}; z)$  of the Matsubara Green's function  $\hat{G}(\mathbf{r}', \mathbf{r}; i\omega_n) = \int_0^\beta \hat{G}(\mathbf{r}', \mathbf{r}; \tau) e^{i(2n+1)\pi T\tau} d\tau$ ,

$$\rho(\mathbf{r}, \omega) = \frac{1}{\pi} \text{Im} \text{Tr} \frac{\hat{1} + \hat{\tau}_3}{2} \left[ \hat{G}(\mathbf{r}, \mathbf{r}; \omega - i\delta) \right]. \quad (26)$$

Using Eqs. (26) and (25), the Fourier transformed fluctuations  $\delta\rho^\pm(\mathbf{q}, \omega)$  in Eq. (20) can be written in the compact form<sup>27</sup>

$$\begin{aligned} \delta\rho^\pm(\mathbf{q}, \omega) &= \\ &\frac{1}{2\pi} \text{Im} \sum_{\mathbf{k}} \text{Tr} \left[ \begin{pmatrix} 1 \\ \tau_3 \end{pmatrix} \hat{G}_0(\mathbf{k}_-, z) \hat{T}(\mathbf{k}_-, \mathbf{k}_+, z) \hat{G}_0(\mathbf{k}_+, z) \right], \end{aligned} \quad (27)$$

where  $\mathbf{k}_\pm = \mathbf{k} \pm \frac{\mathbf{q}}{2}$  and  $z = \omega - i\delta$ . The  $\mathbf{q}$  dependent fluctuation of the LDOS is a probe of all scattering processes combining two momenta  $\mathbf{k}_+$  and  $\mathbf{k}_-$  with a fixed difference  $\mathbf{q}$ .

The only place that a magnetic field enters into the theory, is inside the bare Green-functions, Eq. (24); the effect of the Zeeman splitting on the Green's functions and the  $t$ -matrices can be simply understood as a result of making the substitution

$$\omega \longrightarrow \omega - \hat{\sigma}_3 \mu_B B. \quad (28)$$

This substitution will, in general, modify both the Green's functions and the  $t$ -matrix. Therefore, the breaking of time reversal symmetry can affect the system in two ways: (i) a polarization of the Fermi surface, i.e., a different chemical potential for spin up and down electrons and (ii) for an energy dependent  $t$ -matrix (resonant scatterer), a magnetic field will lead to a difference in the scattering amplitudes of spin up and down electrons.

#### IV. RESULTS

We numerically evaluated  $\delta\rho^\pm(\mathbf{q}, \omega)$  from Eq. (27) using the model (13), considering various different types of impurities. For simplicity, we assumed that the scattering is equal for the two types of electrons 'c' and 'd'.

We computed the Fourier-transformed conductance ratio  $Z(\mathbf{q}, V)|_{\mathbf{q} \neq 0}$  from Eq. (19) by evaluating numerically the fluctuations  $\delta\rho^\pm(\mathbf{q}, \omega)$  from Eq. (27) for potential, magnetic, and resonant scattering. The different types of scattering were modelled using  $t$ -matrices of the form listed in Table I. The computed influence of a magnetic field is illustrated in Figs. 2-4, where  $Z(\mathbf{q}, V)$  is plotted as a function of momentum  $\mathbf{q}$  for two different values of the magnetic field  $B$  at a fixed bias voltage  $eV = \Delta/2$ , where  $\Delta$  is the magnitude of the gap on the electron and hole Fermi surface pockets. ( $\Delta = 0.32t$  in our numerical calculations.) The two chosen values of  $B$  are  $\mu_B B = \Delta$  (upper panels) and  $\mu_B B = \Delta/2$  (lower panels). The voltage  $V$  has been chosen to coincide with the bottom of the quasiparticle gap at the lower field value.

In each of Figs. 2-4, the value of  $Z$  is normalized with respect to its maximum. Furthermore, for a numerical evaluation of the sum over  $\mathbf{k}$  in Eq. (27), we discretized the Brillouin zone in  $N = 10000$   $\mathbf{k}$  points.

##### A. Potential scattering

At first, let us consider the case where the conduction electrons and non-magnetic impurity atoms interact each other via a Coulomb potential. Assuming the Coulomb interaction is screened at length scales comparable to the lattice spacing, we consider a local scattering potential. For a simple modeling of the scattering, we apply Born approximation, which is equivalent to taking only the



first term in Eq. (23). The  $t$ -matrix used in the calculations is

$$\hat{T}_P = \hat{\tau}_3. \quad (29)$$

Figure 2 shows the conductance ratio as a function of wave vector  $\mathbf{q}$ . We obtain a large quasiparticle interference at the  $\mathbf{q}$ -vectors  $\mathbf{q} = (0, \pm\pi)$  and  $\mathbf{q} = (\pm\pi, 0)$  (denoted by  $\mathbf{q}_2$  in Fig. 1) connecting Fermi pockets with opposite sign of SC gap (sign-reversing scattering). The signals for the sign-preserving  $\mathbf{q}$ -vectors  $\mathbf{q} = (\pm\pi, \pm\pi)$  and  $(0, 0)$  (denoted by  $\mathbf{q}_1$  and  $\mathbf{q}_3$  in Fig. 1) are suppressed. The obtained sign change of the SC gap is a characteristic feature of potential scattering which can also be derived from its coherence factor ( $u_{\mathbf{k}}u_{\mathbf{k}'} - v_{\mathbf{k}}v_{\mathbf{k}'}$ ) (compare Table I).

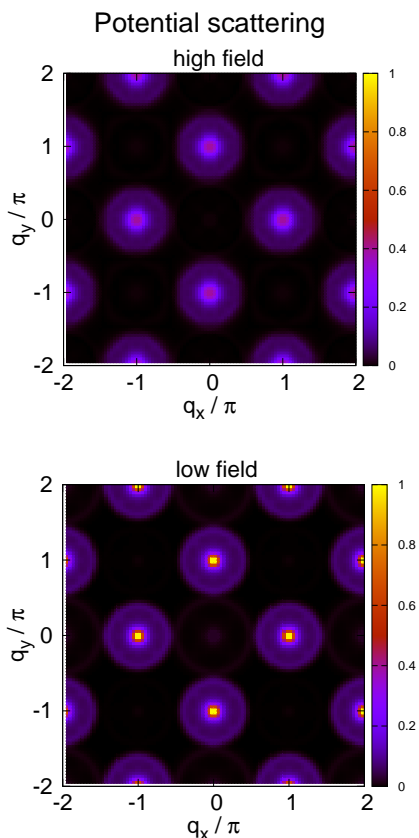


FIG. 2: Normalized conductance ratio  $Z(\mathbf{q}, V)|_{\mathbf{q} \neq 0}$  produced by potential scattering, evaluated at fixed bias voltage  $eV = \Delta/2$ , at “high field”  $\mu_B B = \Delta$  (upper panel) and “low field”  $\mu_B B = \Delta/2$  (lower panel). Potential scattering induces predominantly sign-reversing scattering ( $\mathbf{q} = \mathbf{q}_2$ ), which is suppressed by a field.

As is seen from the upper panel of Fig. 2, a polarization of the Fermi surface by applying a magnetic field does not change the result qualitatively. The intensity of the sign-reversing peaks at  $\mathbf{q}_2$  becomes somewhat smaller with increasing  $B$ . Note that although the Fermi surface

is polarized by the magnetic field, a Coulomb potential is not sensitive with respect to the spin of scattered electrons.

## B. Magnetic scattering

In addition to electrostatic interactions, if the impurity atom has a magnetic moment, there is an exchange interaction between the local spin on the impurity site and the spin of conduction electrons. For the scattering model, we apply again Born approximation and assume a local exchange function. The corresponding  $t$ -matrix that is used in the numerics is

$$\hat{T}_M = \hat{\sigma}_3. \quad (30)$$

Figure 3 presents the conductance ratio for pure mag-

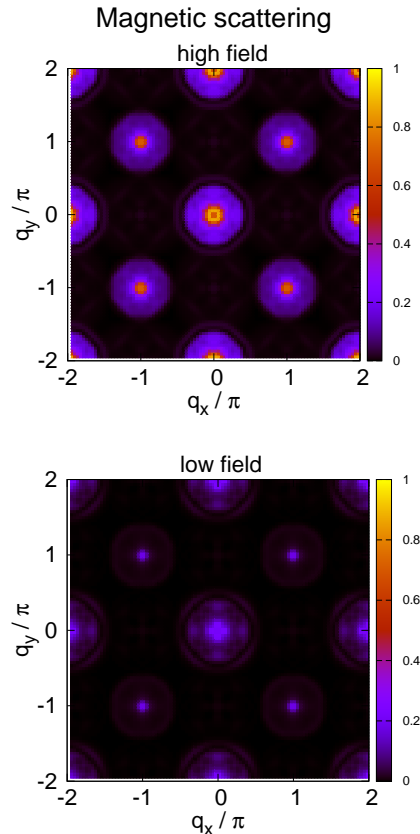


FIG. 3: Normalized conductance ratio  $Z(\mathbf{q}, V)|_{\mathbf{q} \neq 0}$  produced by magnetic scattering, evaluated at fixed bias voltage  $eV = \Delta/2$ , at “high field”  $\mu_B B = \Delta$  (upper panel) and “low field”  $\mu_B B = \Delta/2$  (lower panel). Magnetic scattering induces predominantly sign-preserving scattering ( $\mathbf{q} = \mathbf{q}_{1,3}$ ), which is *enhanced* by a field. Note that in Born approximation, there is no contribution from magnetic scatterers in the zero-field case.

netic scatterers. The quasiparticle interference is enhanced for the sign-preserving scattering processes at  $\mathbf{q}$

vectors  $\mathbf{q}_1$  and  $\mathbf{q}_3$  and the intensity of the peaks is almost equal. On the other hand, sign-reversing processes are suppressed. Furthermore, we obtain a characteristic increase of the peak intensity with increasing values of  $B$ . These results are consistent with other theoretical works that are based on more realistic band models<sup>19, 21</sup>. In the zero-field case,  $B = 0$  LDOS fluctuations coming from magnetic scatterers are suppressed completely. The reason is the proportionality of the scattering potential to the electron spin. Therefore, contributions coming from spin up and down cancel each other when the Hamiltonian is symmetric under time reversal. For  $B > 0$ , where the time reversal symmetry is broken and spin up and down electrons have different chemical potential, coherence factors ( $u_{\mathbf{k}}u_{\mathbf{k}'} + v_{\mathbf{k}}v_{\mathbf{k}'}$ ) associated with a  $t$ -matrix proportional to  $\sigma_3$  lead to sign-preserving scattering. Thus, for magnetic scatterers, the effect of a  $B$  field is driven by a Zeeman-splitting of the bulk superconductor.

### C. Resonant scattering

Resonant scattering is a multiple scattering process, where the main contributions to the  $t$ -matrix derive from higher order terms in which the energy dependence is determined by the bare Green's function  $\hat{G}_0(\mathbf{k}, \omega)$ . The effect of a magnetic field is to replace

$$\omega \longrightarrow \omega - \sigma_3 \mu_B B,$$

inside all Green's functions, and thus a resonant  $t$ -matrix in an external magnetic field  $B$  can be related to the corresponding zero-field form, as follows

$$\hat{T}_R[\omega; B] = T_R[\omega \hat{1} - \mu_B B \hat{\sigma}_3]. \quad (31)$$

An expansion to linear order in the field

$$\hat{T}_R(\omega; B) = T_R(\omega) \hat{1} - T'_R(\omega) B \hat{\sigma}_3 + \dots \quad (32)$$

immediately shows that the leading correction to the zero-field scattering plays the same role as a magnetic impurity. For a phenomenological treatment of resonant scattering, we have taken the form

$$\begin{aligned} \hat{T}_R(\omega; B) &= \frac{1}{(\omega - i\Gamma) \hat{1} - \mu_B B \hat{\sigma}_3} \\ &= \frac{(\omega - i\Gamma) \hat{1} + \mu_B B \hat{\sigma}_3}{(\omega - i\Gamma)^2 - (\mu_B B)^2}, \end{aligned} \quad (33)$$

where we chose the width  $\Gamma$  to be equal to the superconducting gap  $\Delta$  at the Fermi-surface.

The result for  $Z(\mathbf{q}, V)|_{\mathbf{q} \neq 0}$  is shown in Fig. 4. In low field case  $\mu_B B = \Delta/2$  (lower panel), we obtain sign-preserving peaks at  $\mathbf{q} = (0, 0)$  and  $\mathbf{q} = (\pm\pi, \pm\pi)$  of rather weak intensity. Moreover, some slight structures around these peaks appear in the QPI. Increasing the field leads to an enhancement of sign-preserving scattering which

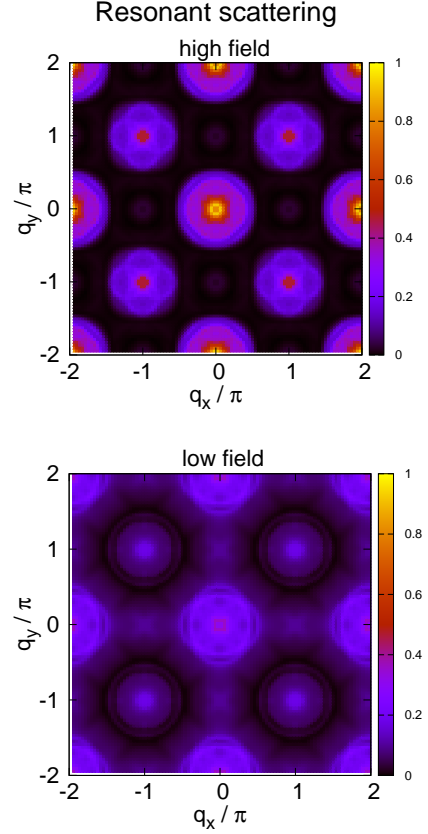


FIG. 4: Normalized conductance ratio  $Z(\mathbf{q}, V)|_{\mathbf{q} \neq 0}$  for resonant scattering, evaluated at fixed bias voltage  $eV = \Delta/2$ , at “high field”  $\mu_B B = \Delta$  (upper panel) and “low field”  $\mu_B B = \Delta/2$  (lower panel). Increasing the field leads to an enhancement of sign-preserving scattering ( $\mathbf{q} = \mathbf{q}_{1,3}$ )

can be seen clearly in the upper panel of Fig. 4 where the intensity of the sign-preserving peaks at  $\mathbf{q} = \mathbf{q}_{1,3}$  is increased noticeably as compared to the lower field case. Moreover, sign-reversing contributions to the QPI become strongly suppressed for higher fields so that we obtain a qualitatively similar picture as for pure magnetic scatterers (compare Fig. 3). This behaviour is also expected from the  $t$ -matrix model (33) which predicts for large enough field values a dominant term proportional to  $\hat{\sigma}_3$  leading to sign-preserving scattering.

### D. Discussion

The results in Figs. 2-4 show a characteristic finite width of  $\Delta q \approx 0.2\pi$  for all QPI peaks. This property is determined by the nesting for scattering processes between the different Fermi surfaces (compare Fig. 1). With Ref.<sup>29</sup> in mind we note that the sign preserving QPI peaks at  $\mathbf{q}_3$  might be very sharp, since the nesting condition is perfectly fulfilled for intrapocket scattering.

In the present work, we have neglected all orbital ef-

fects of the magnetic field on the quasiparticle interference. In order to justify this approximation, we recalculated the conductance ratio for all kinds of scattering under the assumption that the magnetic field is now coupled to the degenerate  $d_{xz}$  and  $d_{yz}$  orbitals within a simplified two orbital model for iron-based superconductors.<sup>30</sup> As a main result, we found that a magnetic field of the order of  $\Delta$  which is coupled to the orbitals leads to a slight deformation of the Fermi surface giving rise to a small change of the nesting conditions. In all cases of scattering, the orbital coupling affected rather the shape than the intensities of the quasiparticle interference peaks which justifies the assumption that the orbital effect in Pauli-limited superconductors is very small in comparison to the field effect based on Zeeman splitting.

## V. CONCLUSIONS

To summarize, we have modelled the effect of Zeeman splitting on quasiparticle interference in iron-based superconductors using an  $s_{\pm}$ -wave-symmetry of the superconducting order parameter. Our model is applicable under the assumption that these superconductors are Pauli limited. We investigated three cases of scattering: The effect of a spin-split spectrum on scattering off (i)

nonmagnetic potential scatterers, (ii) magnetic impurities, and (iii) nonmagnetic resonant scatterers. While the field has almost no effect on scattering off potential impurities, in the cases (ii) and (iii), the main effect of the field is to enhance time reversal odd scattering, enhancing the sign-preserving points and depressing sign-reversing points in the QPI pattern. A possible scattering model that would be in accordance with STM experiments recently performed on the chalcogenide superconductor Fe(Se,Te) consists of potential impurities and resonant scatterers. However, so far there is no direct experimental evidence for the presence of resonant scatterers in these fully gapped superconductors. Possible other effects that arise from breaking the time reversal symmetry such as the influence of a supercurrent on non-magnetic scatterers is an interesting open question that deserves future investigation.

## Acknowledgments

The authors would like to thank T. Hanaguri and H. Takagi for discussions related to this work. This work was supported by DFG grant SY 131/1-1 (SS) and DOE grant DE-FG02-99ER45790 (PC).

- 
- <sup>1</sup> Y. Kamihara, T. Watanabe, M. Hirano, H. Hosono, *J. Am. Chem. Soc.* **130**, 3296 (2008).
  - <sup>2</sup> Z.-A. Ren *et al.*, *Chinese Phys. Lett.* **25**, 2215 (2008).
  - <sup>3</sup> J. W. Lynn, P. Dai, *Physica C* **469**, 469 (2009).
  - <sup>4</sup> I. I. Mazin, D. J. Singh, M. D. Johannes, M. H. Du, *Phys. Rev. Lett.* **101**, 057003 (2008).
  - <sup>5</sup> K. Kuroki *et al.*, *Phys. Rev. Lett.* **101**, 087004 (2008).
  - <sup>6</sup> F. Wang, H. Zhai, Y. Ran, A. Vishwanath, D.-H. Lee, *Phys. Rev. Lett.* **102**, 047005 (2009).
  - <sup>7</sup> V. Cvetkovic, Z. Tesanovic, *EPL* **85**, 37002 (2009).
  - <sup>8</sup> K. Kuroki, R. Arita, *Phys. Rev. B* **64**, 024501 (2001).
  - <sup>9</sup> C. C. Tsuei, J. R. Kirtley, *Rev. Mod. Phys.* **72**, 969 (2000).
  - <sup>10</sup> C.-T. Chen, C. C. Tsuei, M. B. Ketchen, Z.-A. Ren, Z. X. Zhao, *Nature Phys.* **6**, 260 (2010).
  - <sup>11</sup> J. E. Hoffman *et al.*, *Science* **297**, 1148 (2002).
  - <sup>12</sup> K. McElroy *et al.*, *Nature* **422**, 592 (2003).
  - <sup>13</sup> T. Hanaguri *et al.*, *Nature Phys.* **3**, 865 (2007).
  - <sup>14</sup> Y. Kohsaka *et al.*, *Nature* **454**, 1072 (2008).
  - <sup>15</sup> T. Hanaguri *et al.*, *Science* **323**, 923 (2009).
  - <sup>16</sup> T. Hanaguri *et al.*, *Science* **328**, 474 (2010).
  - <sup>17</sup> F. Wang, H. Zhai, D. H. Lee, *EPL* **85**, 37005 (2009).
  - <sup>18</sup> Y. Bang, H. Y Choi, H. Won, *Phys. Rev. B* **79**, 054529 (2009).
  - <sup>19</sup> Y. Y. Zhang *et al.*, *Phys. Rev. B* **80**, 094528 (2009).
  - <sup>20</sup> E. Plamadeala, T. Pereg-Barnea, G. Refael, *Phys. Rev. B* **81**, 134513 (2010).
  - <sup>21</sup> A. Akbari, J. Knolle, I. Eremin, and R. Moessner, *Phys. Rev. B* **82**, 224506 (2010).
  - <sup>22</sup> M. Tinkham, *Introduction to Superconductivity*, 2nd ed. (Dover, New York, 2004).
  - <sup>23</sup> R. Balian and N. R. Werthammer, *Phys. Rev.* **131**, 1553 (1963).
  - <sup>24</sup> A. V. Balatsky, I. Vekhter, and J.-X. Zhu, *Rev. Mod. Phys.* **78**, 373 (2006).
  - <sup>25</sup> P. J. Hirschfeld, D. Vollhardt, and P. Woelfle, *Solid State Commun.* **59**, 111 (1986).
  - <sup>26</sup> D. J. Singh and M.-H. Du, *Phys. Rev. Lett.* **100**, 237003 (2008).
  - <sup>27</sup> M. Maltseva and P. Coleman, *Phys. Rev. B* **80**, 144514 (2009).
  - <sup>28</sup> O. Fischer, M. Kugler, I. Maggio-Aprile and Ch. Berthod, *Rev. Mod. Phys.* **79**, 353 (2007).
  - <sup>29</sup> I. I. Mazin, D. J. Singh, *Comment on "Unconventional s-wave superconductivity in Fe(Se,Te)"*, arXiv:1007.0047.
  - <sup>30</sup> S. Raghu *et al.*, *Phys. Rev. B* **77**, 220503(R) (2008).